

# Seismic Design Method For Railway Structures

Mr. Niteen Nandkishor Chavan<sup>1</sup>, Prof. Mrs. Pallavi K. Pasnur<sup>2</sup>

<sup>1, 2</sup>Dept of ME-Structural Engineering

<sup>1, 2</sup>JSPM's ICOER, Wagholi, Pune – 412 207

**Abstract-** *The design and detailing of rail viaducts for high seismic loads presents several unique challenges that are often not covered adequately by codes of practice. For instance, designers must consider the impact of the natural frequency of the structure on the safety of the train itself. The following paper outlines a practical design approach for designing typical long, multiple span, simply supported concrete viaducts for seismic events. It considers a staged design approach where the safety of the train can be guaranteed under a so-called Level 1 earthquake and the safety of the viaduct structure is checked under a higher Level 2 earthquake. The paper provides a detailed insight into the benefits of using a push over method that accounts for the ductility of the viaduct piers over a more standard force-based approach. This study proposes an approach for developing seismic fragility models based on elastic net regularized logistic regression and applies it to railway bridge classes. Railway bridge class fragilities are not available in the literature despite recorded evidence of earthquake damage to railway bridges. The introduction of elastic net regularization helps in selecting the best set of predictor variables for fragility modeling even if they are mutually correlated. The proposed fragility models are compared to their corresponding highway bridge counterparts, given that current practice in regional risk assessment recommends adopting these as proxies for railway bridge fragility. The analysis reveals that multi span simply supported Railway Bridge, the most common bridge class, and show lower fragility than their corresponding highway bridge counterparts.*

## I. INTRODUCTION

In principle, when an earthquake fault ruptures and propagates towards a site at a speed close to the shear wave velocity, the generated waves will arrive at the site at approximately the same time. This creates the cumulative effect of almost all of the seismic energy radiation from fault and generates a “distinct” velocity pulse within the ground motion time history, at a strike-normal direction.

Bridges are accounted as key transportation infrastructures which their construction impose considerable costs on road and railway projects. In addition, because of their special structural system, they considered to be the most vulnerable element in a roadway or a railway system. One of the suggested structural systems which have achieved more attraction by designers for its use in various practices as culverts, underpasses, overpasses and railway and roadway bridges in recent three decades is soil-steel structures. One of the important issues related to this kind of structures, is their proper and accurate design against the applied loads and particularly the earthquake effects.

## II. CASE STUDY

Basic Parameters of Vehicle-Bridge System. A case study bridge model is used to explore the forward directivity on the seismic response of the bridge. The adapted case study is a typical multi span simply supported boxing bridge under high-speed trains. This bridge type represents more than 90% of China's high-speed railway bridge. The bridges are located in designs that comply with the Temporary Provisions of Newly-Built 300–350 km/h Passenger Special Railway Bridge Design. The cross-sectional dimensions of the Boxing girder and bridge piers of a chosen five-span simply supported bridge for this study can be seen in Figure 2.1. The related parameters are listed below. The bridge consists of five 32 m spans of PC box girders, the piers are 10–20 m high, with round-end sections and pile foundations. Mounted on the piers are fixed pot neoprene bearings. All the piers are cast in situ and concrete strength grade is M35 (the Young's modulus is 3.15 E4 N/mm<sup>2</sup>), longitudinal reinforcement ratio of cross-section is 0.43%. Poisson's ratio  $\nu = 0.2$ . Geometric constants of model boxing girders and round-shaped solid pier are seen in Tables 1 and 2. The secondary dead load (i.e., slab ballast less track structure, =184 kN/m) regarded as the participating vibration mass is spreaded over the boxing girder. The 3D bridge model was developed, and the elastic-plastic analysis of the bridge under high-speed vehicles in this study is conducted based on the second development. The ground motions are all scaled to suit the high level of earthquake for the bridge structure and then input into the structure in order to compute structural nonlinear seismic response.

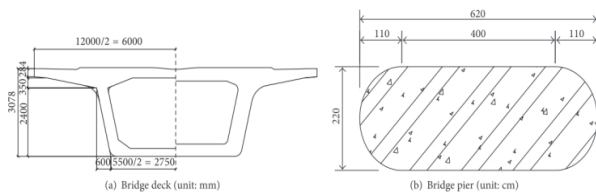


**Fig.2.1 Cross-section of bridge deck and pier**

Length of girder/(m)	Height of girder/(m)	Deck width/(m)	Area of girder/(m <sup>2</sup> )	$I_{yy}$ of girder/(m <sup>4</sup> )	$I_{zz}$ of girder/(m <sup>4</sup> )	Linear mass of girder/(kg/m)
32	3.05	12	8.6597	10.811	80.945	$2.19 \times 10^4$

**Table.2.1 Geometric constants of model boxing girders**

Area of pier (m <sup>2</sup> )	$I_{yy}$ of pier/(m <sup>4</sup> )	$I_{zz}$ of pier/(m <sup>4</sup> )
11.141	3.4515	29.351

**Table.2.2 Geometric constants of model round-shaped solid pier**

The high-speed trains are employed as vehicles live load. With more significant 30 s of registration, the horizontal and vertical ground motion components of the near-fault ground motions considered in the analysis are shown. Take a 14 m pier height as an example to analyze the natural vibration characteristics of the bridge system by an eigenvalue analysis. The foundational period ( $T$ ) of vibration corresponding to the five-span high-speed railway bridge is 0.259 s. This amounts to be less than the pulse periods ( $TP$ ) of the FD pulse ground motions; that is, the bridge can then be labeled a short period structure. Research and experimental results show that the base of the piers will step into the nonlinear stage under high-level earthquake. The elastic-plastic method is used to analyze the seismic responses under high-level earthquake. Elastic-plastic deformation of pier bottom can be calculated by means of the moment-curvature relationship program.

### III. THREE DIMENSIONAL MODELLING

#### 3.1 Geometry of Model and Material Properties-

In 3D state, the perpendicular dimension to the plane, based on Iran Railway geometric design code (2004), is taken equal to 6 m which is according to one way railway track specifications. All material constitution law and their parameters for steel and concrete are the same as 2D condition. Drucker-Prager parameters are calculated using 3D equations.

#### 3.2 Model Elements and Boundary Conditions-

In developed three-dimensional model, bottom of model is constrained in vertical ( $y$ ) and transverse ( $z$ ) directions. In the cases which transverse earthquake

component has applied, longitudinal constrained is also considered. Lateral surfaces of model are constrained by spring-dashpot. Spring stiffness and dashpot damping coefficient are considered as 2D model. In 3D state, two kinds of elements are used. For steel plate meshing, S4R element which is a 4-node, quadrilateral, stress/displacement shell element is used. In addition, soil and abutments are discretized using C3D8R which is a solid 8-node linear brick element.

#### 3.3 Loading and Constrains-

The loading in seismic analyses of structures in time domain is usually defined by imposing the earthquake acceleration time history on the model base. In this order, longitudinal component of NIS station accelerogram of Kobe (1995) earthquake (Figure 3.3.a) with PGA 0.51g is selected and applied on the model base in x direction of structure while its transverse component (Figure 3.3.b) with PGA 0.48g is applied in z direction. In 2D model only the longitudinal component of accelerogram is implemented. In this study, the vertical component of earthquake is neglected. In part of study, to survey the effect of acceleration amplitude, accelerogram is scaled for three acceleration 0.25g, 0.35g and 0.45g.

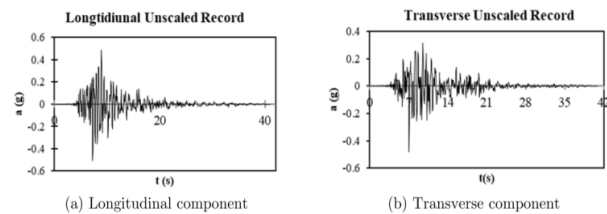


**Fig.3.3 Cross-section of bridge deck and pier**

#### 3.4 Sensitivity Analysis Results-

With regard to mentioned theme in literature review, it was clarified that in seismic behavior of soil-steel bridges, various subjects as predomination of 2D or 3D behavior, shape and geometry of bridge (i.e. arch or box), linear and nonlinear behavior of material and effects of earthquake excitation have not perused. In order to perform a rather comprehensive study through the lens of this viewpoint, following parameters are used for performing sensitivity analysis:

1. Geometry of soil steel bridge structure (4 types of arch structure)
2. Elastic and elasto-plastic behavior of soil
3. Soil cover height

4. Effect of simultaneity of longitudinal and transverse component of earthquake waves
5. Effect of earthquake wave approach to structure
6. The difference between results of 2D and 3D numerical models

### 3.5 Effect of Material Behavior on Results of 2D and 3D Models-

In order to scrutinize the effects of sensitivity analysis on internal forces, variation diagram of these forces are plotted for 2D and 3D models in linear and non-linear conditions. In 3D models, internal forces values are extracted in three sections of  $z = 0\text{ m}$ ,  $z = 3\text{ m}$  and  $z = 6\text{ m}$ . Comparing values in these three sections shows that the first and the third sections' values are the same and greater than the second section. However, axial force variation procedure in medial section is different from two other sections, but its maximum values are smaller. Therefore, in 3D models, internal forces are extracted in the third section  $z = 6\text{ m}$ . All values are recorded in time corresponding to maximum acceleration of input accelerogram. Figure 3.5 shows variation of internal forces with respect to span length for 0.25g PGA and for two spans  $14.13\text{ m} \times 7.6\text{ m}$  and  $23.40\text{ m} \times 11.70\text{ m}$ .

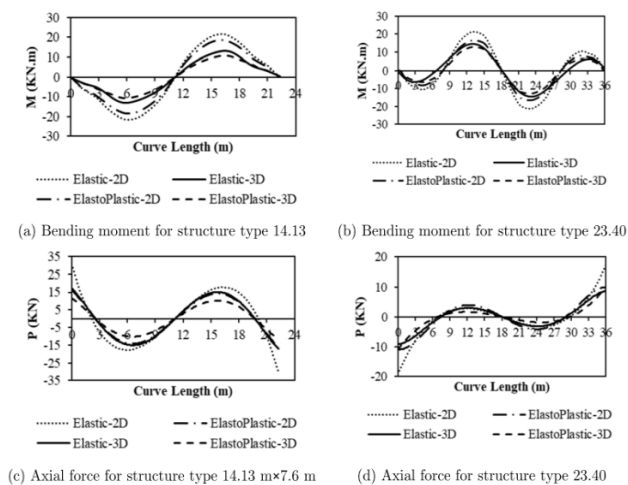


**Fig.3.5 Internal forces diagrams for PGA 0.25g for structure types  $14.13\text{ m} \times 7.6\text{ m}$  and  $23.40\text{ m} \times 11.7$**

According to Figure 3.5 and other diagrams for all structures' dimensions and accelerations, values of internal forces in 3D state with elasto-plastic behavior are smaller than other states. For instances, maximum moments corresponding to PGA 0.25g and for structure type  $14.13\text{ m} \times 7.6\text{ m}$  in 3D elasto-plastic state is 19% smaller than moment value in 3D elastic model. The relative difference of shear and axial forces are 16% and 43%, respectively. Also, relative difference between elasto-plastic 2D and 3D corresponding to PGA 0.25g for bending moment, shear and axial force are 36%,

23% and 21%, respectively. The mentioned relative differences corresponding to PGA 0.45g for bending moment, shear and axial force are 37%, 22% and 28%, respectively. Hence, as it was observed, except for PGA 0.25g, for two other PGA values maximum difference between elasto-plastic 2D and 3D belongs to maximum bending moment. This difference can be explained in such way that in 2D state, force distribution in direction of perpendicular to the bridge plane is not possible; as a consequence, one section of steel plate must tolerate all forces, while in 3D state load distribution occurs in lateral direction and various sections in width of bridge will participate in load carrying. On the other side, occurring permanent plastic deformation in elasto-plastic behavior absorbs earthquake energy and consequently decreases internal forces in steel arch.

### IV. EFFECT OF EARTHQUAKE WAVE ANGLE OF APPROACH ON RESULTS 3D MODELS

In the real situation, it is possible for a structure to be subjected to earthquake waves in any angle. Whereof in nonlinear behavior of structure and its surrounding soil, the superposition principle is not valid; therefore, decomposition of earthquake force and then applying components in arbitrary direction and finally linear summation of results is not correct approach. Therefore, effect of this phenomenon will be studied in this section. The Kobe earthquake has two longitudinal and transverse accelerogram, in order to change the approaching angle of waves; rotation matrix is used. In order to survey effect of impact angle of earthquake, diagram of internal forces for 3D model and elasto-plastic behavior in 3 sections  $z = 0\text{ m}$ ,  $z = 3\text{ m}$  and  $z = 6\text{ m}$  are plotted. Figure 4.1 shows internal forces with respect to length curve in structure type  $14.13\text{ m} \times 7.6\text{ m}$  for PGA 0.45g, soil cover 1.5m and for impact angle of 0, 30, 60 and 90 degrees in section  $z = 0\text{ m}$ . Also, Figure 4.2 shows same parameters in structure type  $23.40\text{ m} \times 11.70\text{ m}$  with the same conditions.

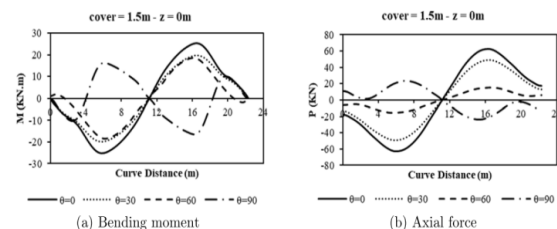


**Fig.4.1 Variation of internal forces respect to curve length for 0.45g PGA in structure type  $14.13\text{ m} \times 7.6\text{ m}$  arch**

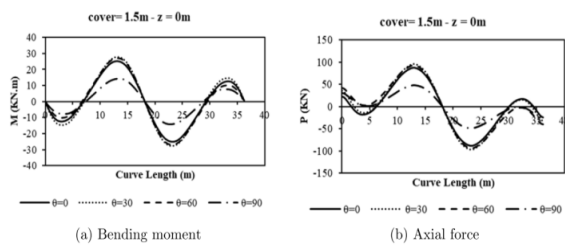


**Fig.4.2. Diagram Variation of internal forces with respect to curve length for 0.45g PGA in structure type 23.40 m×11.70 m arch**

As it was observed, for soil cover 1.5 m, maximum values of bending moment, shear and axial force are happened in  $\theta = 0^\circ$ , whereas for structure type 23.40 m×11.70 m this angle is 30 degree. Also, it is worth mentioning that in structure type 14.13 m×7.6 m with changing impact angle to 90 degree, pattern of bending moment, shear and axial force changes, since in structure type 23.40 m×11.70 m the values of internal forces are close together. While on the contrary, for soil cover 2.5m and 3.5m these values for different angles change and it is not possible to denote an angle in which internal forces are maximized. Furthermore, comparison between variation pattern of axial force in different sections in two types of structures shows that for first and last sections ( $z = 0$  m and  $z = 6$  m) the variation pattern are similar, but, in middle section ( $z = 0$  m) this pattern is different, while the variation pattern for bending moment and shear force in all sections are the same. In conclusion, from internal force point of view, analysis under impact angle of  $\theta = 0^\circ$  yields to critical results.

## V. CONCLUSION

In this paper, the effects of earthquake loading on soil-steel structure were studied. In this order by using 2D and 3D model of these kinds of bridges were developed and dynamic analyses were performed under Kobe earthquake input motion. Sensitivity analyses were executed on parameters like soil cover height, structure geometry, PGA value, elastic and elasto-plastic material behavior and 2D and 3D geometry of structures. A summary of most important findings of numerical study can explained as follows:

1. Values of internal forces of 2D models are smaller than corresponding values in 3D models. Maximum values of internal forces for various spans and PGA, elastic and elasto-plastic behavior in 2D condition is 2% to 57% greater than 3D condition.
2. The maximum values of internal forces for various spans and PGAs for both elastic and elasto-plastic behavior, in 2D models are 2% to 57% smaller than

3D models. Also, internal forces values obtained from elasto-plastic analysis are smaller than elastic ones.

3. The maximum values of bending moment for all spans and PGAs, for 2D and 3D models in elastic behavior are 12% to 40% greater than elasto-plastic behavior. These variations for axial and shear forces are 10% to 30% and 12% to 68%, respectively.
4. Increase in soil cover height from 1.5m to 3.5m causes increase in internal forces value of steel plate between 2% to 59%.
5. Generally, by increasing PGA, maximum internal forces increase. This increase is different for various arch dimensions and depends on 2D and 3D modeling and elastic and elasto-plastic behavior. The ranges of these variations are between 30% and 50%.
6. In general, by changing impact angle of earthquake waves from 0 to 90, no regular pattern found for variation of internal forces.
7. Comparison of buckling ratio variation due to impact angle changes shows that for all spans and soil covers, increase in impact angle yields to decrease in buckling ratio. The range of this reduction is from 13% to 59%.

## REFERENCES

- [1] AASHTO. (2017). LRFD Bridge Design Specifications. American Association of State Highway and Transportation Officials, Washington, D.C.
- [2] ABAQUS. (2010). "Abaqus Online Documentation." assault Systèmes Simulia Corp, RI, USA.
- [3] Ai-lan, C., Takahiro, I., and Xiu-run, G. (2006). "Study on Dynamic Response of Embedded Long Span Corrugated Steel Culverts using Scale Model Shaking Table Tests and Numerical Analyses." Journal of Zhejiang University, 7(3), 430–435.
- [4] AS/NZS 2041. (2011). Buried Corrugated Metal Structures. Sydney, NSW.
- [5] ASTM. (2006). ASTM A796 / A796M-06, Standard Practice for Structural Design of Corrugated Steel Pipe, Pipe-Arches, and Arches for Storm and Sanitary Sewers and Other Buried Applications, West Conshohocken, PA.
- [6] CHBDC. (2014). CSA S6-14 – Canadian Highway Bridge Design Code. Rexdale Toronto.
- [7] Day, R. W. (2002). Geotechnical earthquake engineering handbook. McGraw-Hill New York.
- [8] Esmaeili, M., and Abdulrazagh, P. (2010). "Pseudo-static evaluation of earthquake effects on soil steel bridges."
- [9] Esmaeili, M., Zakeri, J. A., and Abdulrazagh, P. H. (2013). "Minimum depth of soil cover

above long-span soil-steel railway bridges.” International Journal of Advanced Structural Engineering.”